

Supporting Information for

## Hetero-Interfaces on Cu Electrode for Enhanced Electrochemical Conversion of CO<sub>2</sub> to Multi-Carbon Products

Xiaotong Li<sup>1, #</sup>, Jianghao Wang<sup>1, #</sup>, Xiangzhou Lv<sup>1</sup>, Yue Yang<sup>1</sup>, Yifei Xu<sup>1</sup>, Qian Liu<sup>1</sup>, Hao Bin Wu<sup>1, \*</sup>

<sup>1</sup> Institute for Composites Science Innovation (InCSI) and State Key Laboratory of Silicon Materials, School of Materials Science and Engineering, Zhejiang University, Hangzhou 310027, P. R. China

<sup>#</sup> Xiaotong Li and Jianghao Wang contributed equally to this work.

\*Corresponding author. E-mail: [hbwu@zju.edu.cn](mailto:hbwu@zju.edu.cn) (Hao Bin Wu)

### Supplementary Figures and Tables

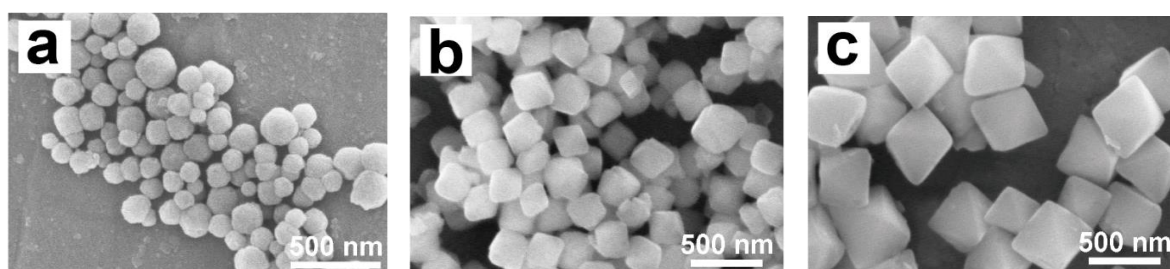


**Fig. S1** SEM images of UiO-66 with different sizes of (a) 100 nm, (b) 300 nm, and (c) 600 nm

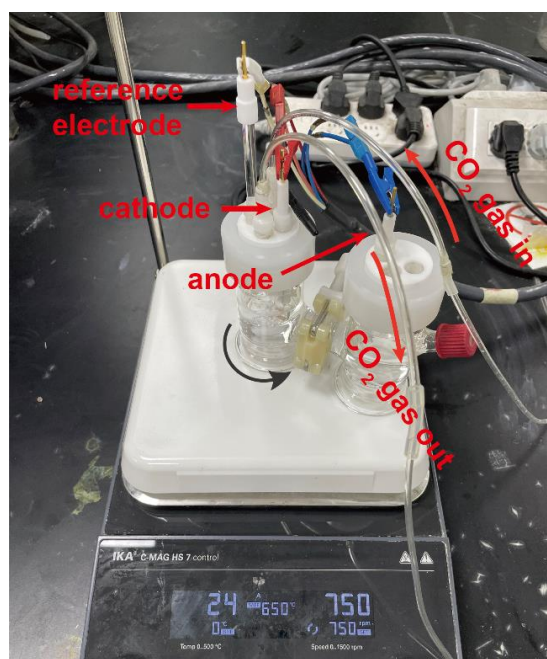


**Fig. S2** Photo of the H-cell setup used in this work

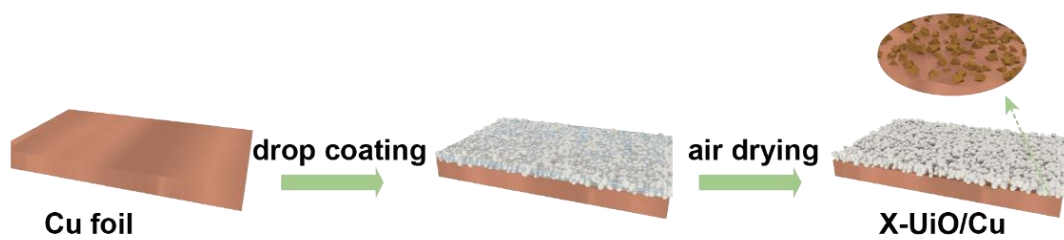


**Fig. S3** Schematic of the synthetic process of UiO-66 modified Cu foil (X-UiO/Cu)

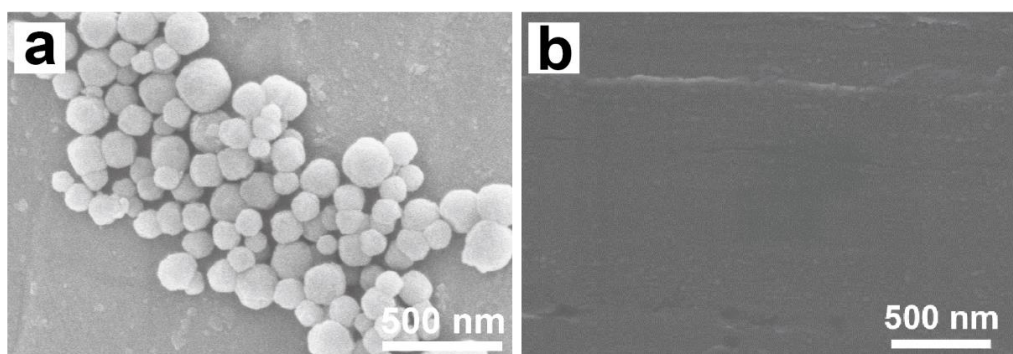


**Fig. S4** SEM images of (a) UiO-66 nanoparticles and (b) mechanically polished Cu foil

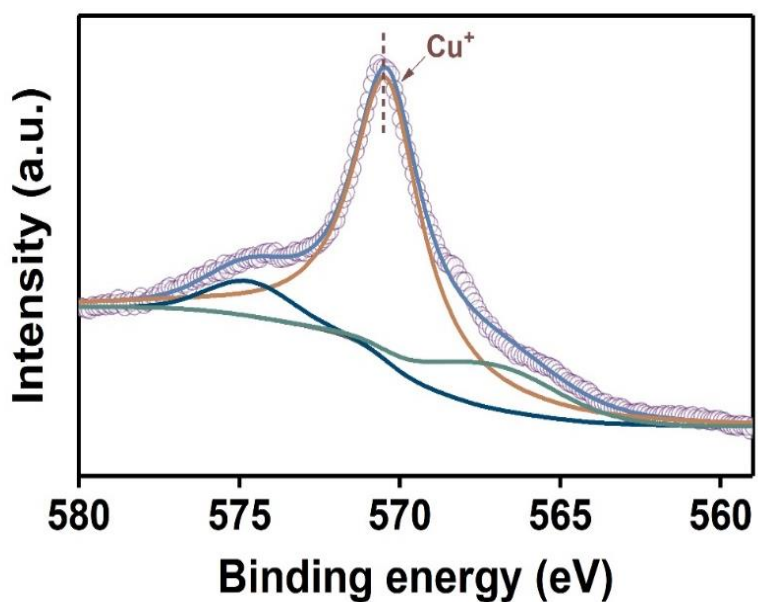


**Fig. S5** Cu LMM AES spectrum of 0.5-UiO/Cu-bare before CO<sub>2</sub>RR

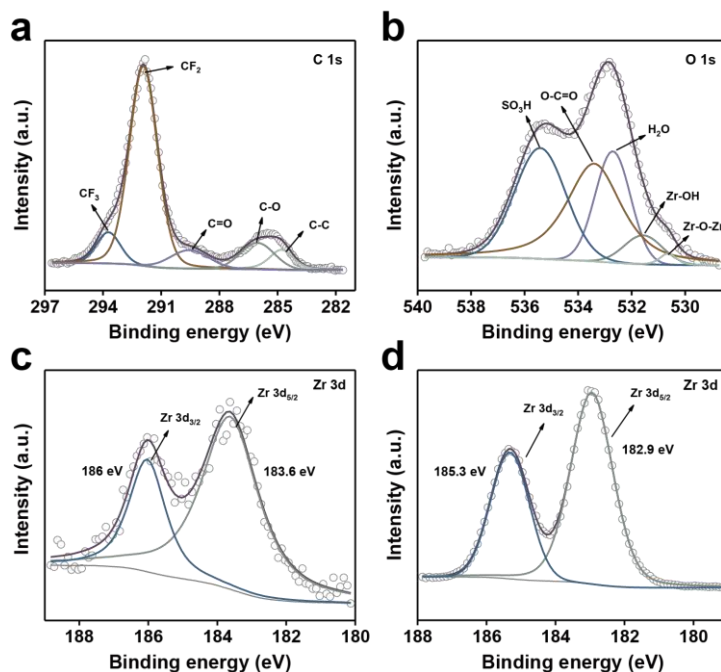


**Fig. S6** (a) C 1s XPS spectrum, (b) O 1s XPS spectrum and (c) Zr 3d XPS spectrum of 0.5-UiO/Cu. (d) Zr 3d XPS spectrum of UiO-66 nanoparticles. All samples in Fig. S6 are characterized before CO<sub>2</sub>RR

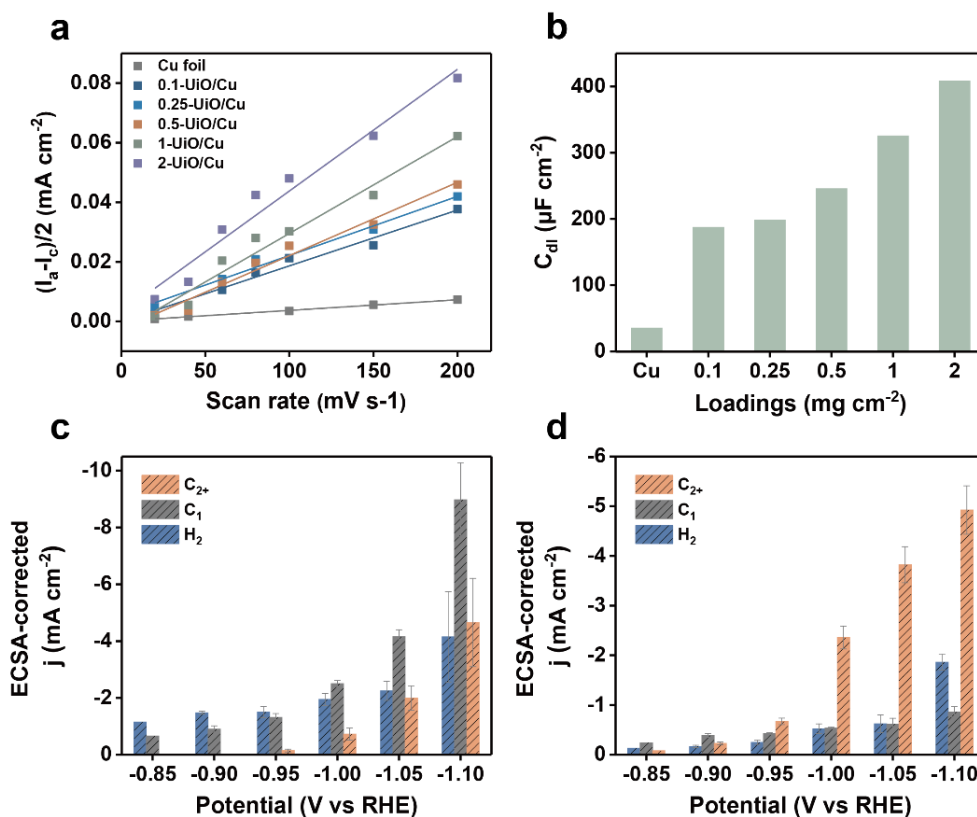


**Fig. S7** (a) Linear fitting of capacitive currents and (b) the corresponding electrochemical double-layer capacitance ( $C_{dl}$ ) (the slopes of the fitting curves in (a)) of X-UiO/Cu. The ECSA-corrected current density for H<sub>2</sub>, C<sub>1</sub>, and C<sub>2+</sub> products as a function of potential on (c) Cu and (d) 0.5-UiO/Cu

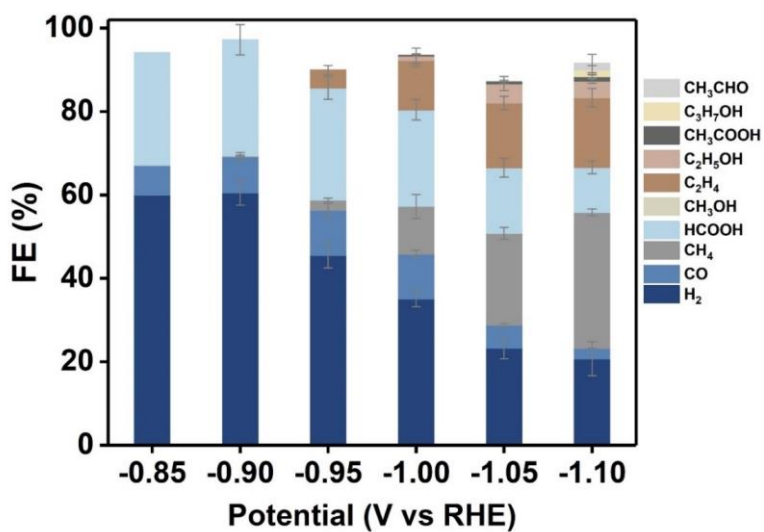


**Fig. S8** FEs of CO<sub>2</sub>RR and HER products on Cu foil as a function of potential

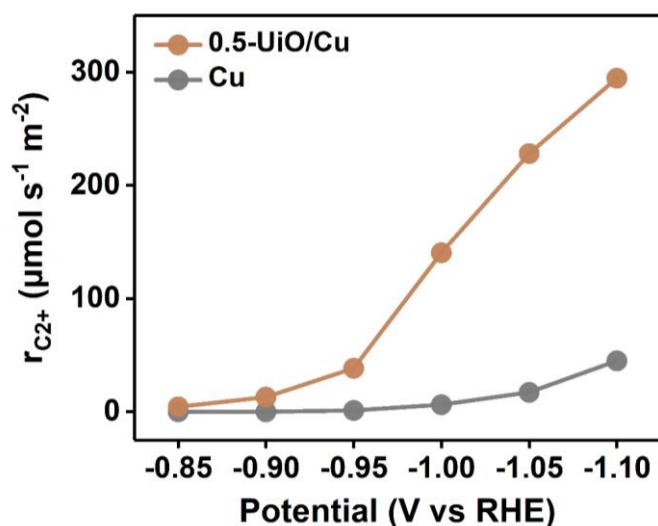


**Fig. S9** Formation rates of C<sub>2</sub>+ products ( $r_{C2+}$ ) on Cu foil and 0.5-UiO/Cu as a function of potential

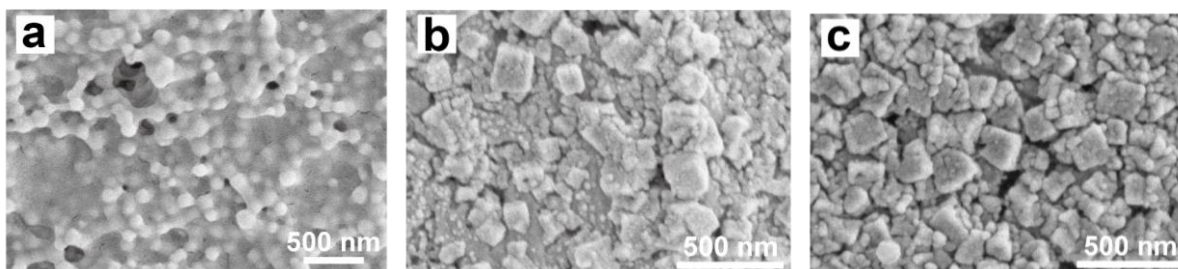


**Fig. S10** Top-view SEM images of 0.5-UiO/Cu electrode after CV: (a) with and (b) without the surface coating layer. (c) Top-view SEM image of 0.5-UiO/Cu electrode after CA without the surface coating layer

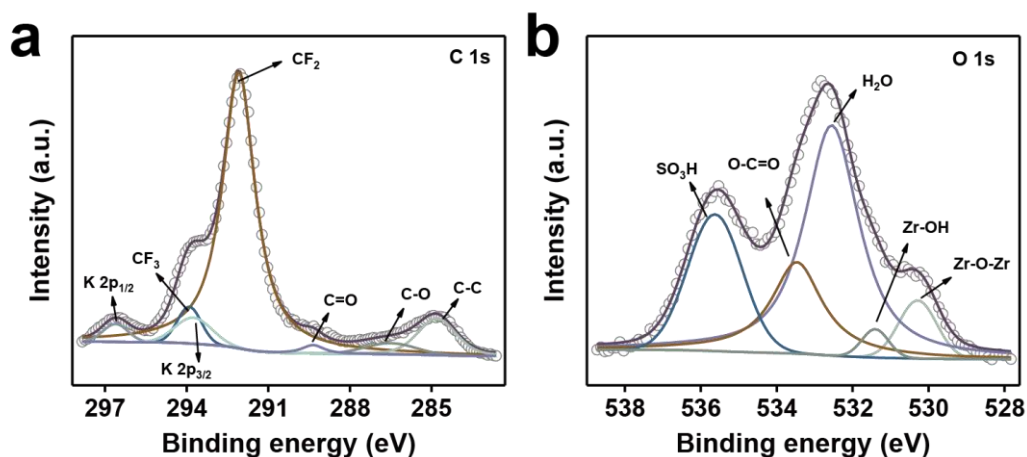


**Fig. S11** (a) C 1s spectrum and (b) O 1s spectrum of 0.5-UiO/Cu after  $CO_2RR$  at -1.05 V vs. RHE for 1 h

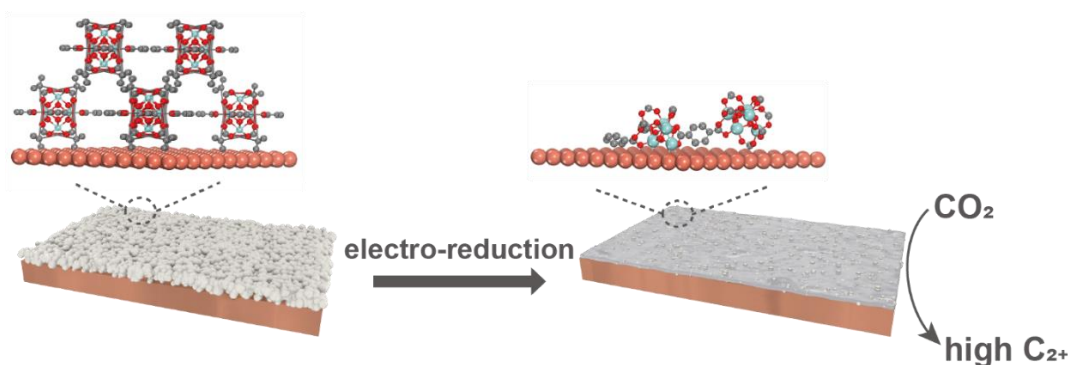


**Fig. S12** Schematic of possible evolution process of UiO-66 coating on X-UiO/Cu electrode under  $CO_2RR$

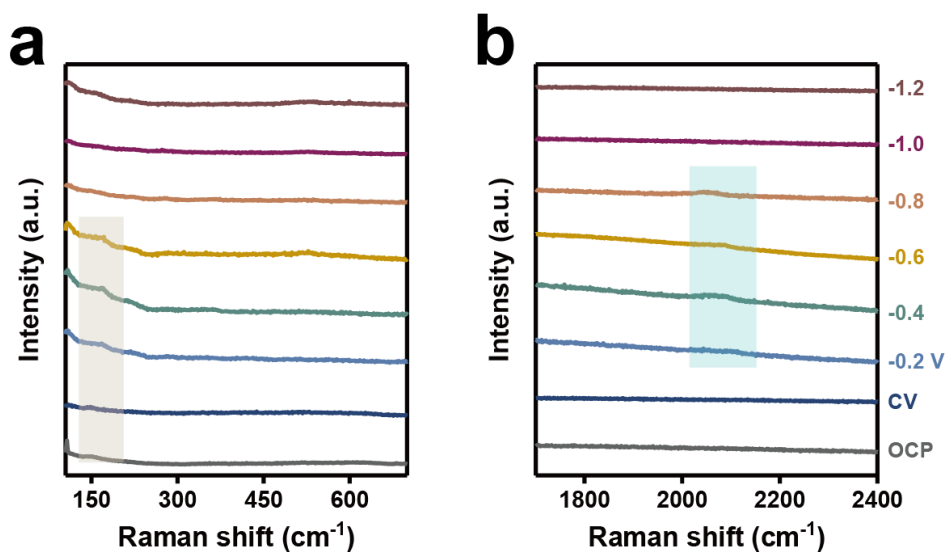


**Fig. S13** The *in situ* surface-enhanced Raman spectra recorded between (a) 100-700  $cm^{-1}$  and (b) 1700-2400  $cm^{-1}$  on Cu foil at OPC, after CV, and at the selected potential range of -0.2 V to -1.2 V vs. RHE with a potential interval of 0.2 V for 10 min

**Table S1** The  $C_{dl}$ ,  $R_f$ ,  $ECSA$ , and  $ECSA$ -corrected  $j_{C^{2+}}$  of Cu and X-UiO/Cu

<b>Sample</b>	<b><math>C_{dl}</math> (<math>\mu F\ cm^{-2}</math>)</b>	<b><math>R_f</math></b>	<b><math>ECSA</math></b>	<b><math>ECSA</math>-corrected <math>j_{C^{2+}}</math></b>
Cu	35.37	1	1	1.99
0.1-UiO/Cu	187.39	5.3	5.3	1.76
0.25-UiO/Cu	198.41	5.61	5.61	3.35
0.5-UiO/Cu	245.9	6.95	6.95	3.82
1-UiO/Cu	325.32	9.2	9.2	2.90
2-UiO/Cu	408.26	11.54	11.54	2.45

**Table S2** Comparison of CO<sub>2</sub>RR performance on 0.5-UiO/Cu with state-of-the-art Cu-based catalyst evaluated in H-type cell

Refs.	catalyst	cell type	electrolyte	$E_{we}/(\text{RHE})$	FE of C <sub>2+</sub>	ECSA- collected $j_{C_{2+}}$ (mA cm <sup>-2</sup> )	geometric area normalized $j_{C_{2+}}$ (mA cm <sup>-2</sup> )	$r_{C_{2+}}$ : Formation rate of C <sub>2+</sub> ( $\mu\text{mol s}^{-1} \text{m}^{-2}$ )	stability (h)
<b>This work</b>	<b>0.5-UiO/Cu</b>	<b>H-cell</b>	<b>0.1 M KHCO<sub>3</sub></b>	<b>-1.05</b>	<b>74.17%</b>	<b>-3.822</b>	<b>-26.57</b>	<b>228.08</b>	<b>32</b>
ACS Catal. 2021, 11, 2473-2482	Cu@N <sub>x</sub> C	home-made H-cell	0.1 M KHCO <sub>3</sub>	-1.1	76.8%	-5	-14.9	128.69	2.7
Joule. 2021 5, 429-440	Cu-DS	H-cell	0.1 M KHCO <sub>3</sub>	-1.08	78%	N/A	-23.4	186.56	30
Small. 2021, 2102293	Cu@Ag-2	Flow-cell	1 M KOH	-1.1	67.6%	N/A	-22.7	193.53	14
Nano Res. 2021 doi.org/10.1007/s12274- 021-3532-7	Cu-s	H-cell	0.1 M KHCO <sub>3</sub>	-1.1	55.8%	N/A	-26.69	230.52	8
Electrochim Acta. 2021, 388, 138552	p-Cu	H-cell	0.1 M KHCO <sub>3</sub>	-1.3	57.2%	N/A	-22.65	195.69	10
Green Chem. 2020, 22, 6540-6546	CuO- CeO <sub>2</sub> /CB	H-cell	0.1 M KHCO <sub>3</sub>	-1.1	50%	N/A	-3.77	32.56	9
Angew. Chem. Int. Ed. 2021, 60, 7426-7435	5-Ag/Cu <sub>2</sub> O	H-cell	0.1 M KHCO <sub>3</sub>	-0.98	65%	-0.41	-6.09	51.25	12
Angew. Chem. Int. Ed. 2021, 60, 15344-15347	Cu/CuSiO <sub>3</sub>	H-cell	0.1 M KHCO <sub>3</sub>	-1.1	60.64%	N/A	-12.25	105.80	6
ACS Appl. Nano Mater. 2020, 3, 257-263	Cu GNC-VL	H-cell	0.5 M KHCO <sub>3</sub>	-0.87	70.5%	N/A	-7.33	63.33	12
Chem. Mater. 2020, 32, 3304-3311	Cu <sub>3</sub> N	H-cell	0.1 M CsHCO <sub>3</sub>	-1	68%	-0.714	-12.58	102.15	3.33
ACS Energy Lett. 2021, 6, 437-444	CuBr-DDT	H-cell	0.1 M KCl	-1.25	72%	-8.75	-9.02	76.90	15
ACS Catal. 2020, 10, 4103-4111	Cu/PANI	H-cell	0.1 M KHCO <sub>3</sub>	-1.2	66%	-5.17	-14.9	127.91	20

Some data in **Table S2** is collected from figures in the corresponding literature, which may be less precise.

**Table S3** EDS results of 0.5-UiO/Cu NPs, 0.5-UiO/Cu-CV NPs, and 0.5-UiO/Cu-CA NPs

trail/at%	C	O	Cu	Zr
UiO/Cu NPs	67.89	27.47	0.83	3.80
UiO/Cu-CV NPs	49.71	41.86	1.04	7.39
UiO/Cu-CA NPs	33.71	49.26	2.72	14.32

**Table S4** FEs of H<sub>2</sub> and various CO<sub>2</sub>RR products as well as the geometric current density on Cu foil as a function of potential

E <sub>we</sub> (RHE)	j (mA cm <sup>-2</sup> )	H <sub>2</sub>	CO	CH <sub>4</sub>	HCOOH	C <sub>2</sub> H <sub>4</sub>	C <sub>2</sub> H <sub>5</sub> OH	CH <sub>3</sub> COOH	C <sub>3</sub> H <sub>7</sub> OH	CH <sub>3</sub> CHO
-0.85	1.92	60.01	7.12	0	27	0	0	0	0	0
-0.90	2.45	60.5±2.91	8.69±1.03	0.18±0.18	27.84±3.66	0	0	0	0	0
-0.95	3.29	45.49±2.97	10.86±1.62	2.46±0.44	26.85±2.72	4.3±1.13	0	0	0	0
-1	5.53	35.14±1.99	10.72±0.89	11.4±2.85	23.17±2.44	11.88±1.53	1.06±1.83	0.14±0.25	0	0
-1.05	9.63	23.3±2.52	5.52±0.38	22.01±1.44	15.73±2.22	15.5±1.57	4.66±1.72	0.41±0.36	0	0
-1.1	19.67	20.72±4.04	2.52±0.06	32.59±0.83	10.79±1.48	16.72±2.19	3.99±0.49	1.09±0.40	1.56±1.08	1.57±2.22

**Table S5** FEs of H<sub>2</sub> and various CO<sub>2</sub>RR products as well as the geometric current density on 0.5-UiO/Cu electrode as a function of potential

E <sub>we</sub> (RHE)	j (mA cm <sup>-2</sup> )	H <sub>2</sub>	CO	CH <sub>4</sub>	HCOOH	CH <sub>3</sub> OH	C <sub>2</sub> H <sub>4</sub>	C <sub>2</sub> H <sub>5</sub> OH	CH <sub>3</sub> COOH	C <sub>3</sub> H <sub>7</sub> OH	CH <sub>3</sub> CHO
-0.85	3.06	29.16	19.1	0	36.58	0	7.18	7	0	3.94	0
-0.9	5.81	19.94±2.39	17.68±0.91	0	28.73±2.69	0	15.29±1.12	7.07±3.12	0	5.25±0.62	0
-0.95	9.72	17.76±3.47	10.5±1.2	1.33±0.31	18.01±1.91	0.84±0.78	28.44±2.47	9.63±1.02	0.54±0.19	8.68±0.79	0.56±0.47
-1	23.95	15.06±1.85	3.15±0.28	3.38±0.58	8.73±0.99	0.58±0.25	40.68±1.4	16.8±1.33	0.75±0.42	8.21±0.31	1.94±0.93
-1.05	35.78	11.98±2.81	1.41±0.28	4.45±1	5.7±2.07	0.53±0.58	42.2±1.92	20.97±0.73	0.86±0.21	8.2±0.25	1.95±0.63
-1.1	56.71	22.88±1.48	0.83±0.19	6.35±0.9	3.06±0.55	0.5±0.36	33.02±1.77	22.41±2.44	0.5±0.19	3.77±0.74	0.75±0.05



**Table S6** FEs of H<sub>2</sub> and various CO<sub>2</sub>RR products as well as the geometric current density on various X-UiO/Cu electrodes at -1.05 V vs. RHE

Loading (mg cm <sup>-2</sup> )	j (mA cm <sup>-2</sup> )	H <sub>2</sub>	CO	CH <sub>4</sub>	HCOOH	CH <sub>3</sub> OH	C <sub>2</sub> H <sub>4</sub>	C <sub>2</sub> H <sub>5</sub> OH	CH <sub>3</sub> COOH	C <sub>3</sub> H <sub>7</sub> OH	CH <sub>3</sub> CHO
0.1	16.5	15.84	2.25	9.36	10.66	0	33.3	16.32	0.13	5.88	0.92
0.25	26.34	9.45±0.9	1.66±0.14	5.56±0.62	5.91±0.94	0.17±0.3	43.32±2.01	18.39±0.94	0.72±0.18	6.58±0.28	1.77±0.51
0.5	35.78	11.98±2.81	1.41±0.28	4.45±1	5.7±2.07	0.53±0.58	42.2±1.92	20.97±0.73	0.86±0.21	8.2±0.25	1.95±0.63
1	44.34	22.56±2.93	1.49±0.16	4.8±0.97	5.84±1.23	0.7±0.82	34.11±1.6	17.61±1.7	0.75±0.24	6.27±2.94	1.22±0.59
2	56.72	27.36	1.08	4.58	6.08	0.78	27.67	13.3	0.43	8.2	0.32